Temperature and pressure sensitive coatings

J. von Wolfersdorf[1], P. Ott[2] & B. Weigand[1]
[1]*Institut für Thermodynamik der Luft- und Raumfahrt (ITLR), Universität Stuttgart, Stuttgart, Germany.*
[2]*Laboratoire de thermique appliquée et de turbomachines (LTT), Ecole Polytechnique Fédérale de Lausanne (EPFL), Lausanne, Switzerland.*

Abstract

To understand flow and heat transfer phenomena in nature and to use them for design purposes qualitative visualization techniques as well as quantitative full surface measurement methods are required. This paper focuses on two surface coatings to be applied for temperature measurements and full surface pressure indications. The first is related to thermochromic liquid crystals for thermography and the second to pressure sensitive paints. These coatings have been applied for the purposes of visualization and measurement. Both techniques use optical methods to measure the sensor signals. The powerful development in data acquisition hardware and software, computers and digital image processing plays an important role in this context and supports the widespread applicability to a variety of phenomena in nature and design.

1 Introduction

Several substances that are sensitive to temperature or pressure changes, as well as physical effects of colour appearance in nature, have been discovered over time mainly by botanists and zoologists [1, 2]. Some of the effects are related to special materials or states of matter like liquid crystals and luminophores. The distinct properties of these substances, like reflection of polarized light or the influence of luminescent activity by oxygen quenching, have made them very interesting for engineering purposes in thermography and pressure measurements. Engineering and medical applications of these coatings have led to the investigation of their properties, application processes and cost-effective production procedures. In addition, these surface coatings are nowadays 'coming back to nature' in, for example, thermoregulation studies of animals and plants or possibly pressure distribution measurements on insect wings during different flight operations.

WIT Transactions on State of the Art in Science and Engineering, Vol 4, © 2006 WIT Press
www.witpress.com, ISSN 1755-8336 (on-line)
doi:10.2495/1-84564-095-0/7e

2 Thermochromic Liquid Crystals (TLCs)

Liquid crystals are anisotropic materials that exist between the solid phase and the isotropic liquid phase. The temperature visualization capability of TLCs is based on the property of some cholesteric or chiral-nematic liquid crystals to reflect defined colours at specific temperatures and viewing angles. This liquid crystal behaviour occurs in the temperature range where the material undergoes the transition between the solid and the liquid states. The temperature range might be relatively narrow (∼1°C) or broad (∼20°C), depending on specific substances. They are classified as narrow- and wide-band TLCs, respectively. The colour change for TLCs ranges from clear to red as the temperature increases, then to yellow, green, blue and violet before turning again to colourless at the so-called clearing point, where the isotropic phase is reached (Fig. 1).

As organic compounds, liquid crystals have limited working temperature ranges between −30°C and 120°C approximately. The observed colour changes are repeatable and reversible as long as the TLCs are not damaged, e.g. by overheating or excessive UV light exposure. To avoid damaging of the TLCs, especially due to chemical contamination and UV radiation, they are usually encapsulated in 5–10 μm diameter plastic shells. These shells exist in a water-based binder material, which makes the coating sprayable. In addition, the use of TLCs is relatively inexpensive and they are easy to apply. The response time of the TLC is approximately 3 ms [3], which is short enough for typical fluid flow and thermal problems.

During the last few decades, TLCs have been applied to many problems in fluid flow, heat transfer, engineering and medicine. They have been used to investigate electronic components and circuit integrity and to detect surface flaws in structural components. Early studies were related to thermal mapping in aerospace applications and non-destructive testing [4, 5]. Several reviews were given for general fluid flow and heat transfer studies [6, 7], hypersonic flows [8, 9], gas turbine heat transfer [10] including rotating surfaces [11], boiling heat transfer [12], and in measurements of human skin temperature for medical treatment [13–15]. The easy applicability of liquid crystals as a non-invasive method is especially useful for screening large groups of patients [16] and for a variety of medical cases such as breast cancer diagnostics, detection of vascular disorder or neuronal dysfunctions among many others.

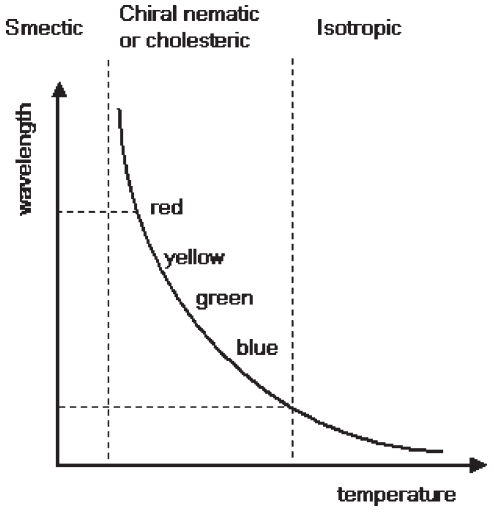

Figure 1: Typical reflected wavelength–temperature response of TLCs.

Although the response of liquid crystals to temperature changes was discovered in 1888 by Friedrich Reinitzer, an Austrian botanist, its widespread use in thermography today is driven mainly by engineering and medical applications. This allowed for the development of cost-effective production procedures for a variety of TLCs and therefore relatively inexpensive application systems. As a safe, non-toxic and user-friendly thermo-optical technique, liquid crystal thermography is nowadays applied to animal thermoregulation studies [17] and full surface temperature mapping of leaves to analyse physiological processes such as photosynthesis and transpiration in plants [18]. Some cases of natural occurrence of cholesteric liquid crystals are known in beetles and spider webs [19, 20]. The most prominent one is in the iridescent outer coatings of several scarabaeid beetles [21]. Figure 2 shows the colours in the exocuticles of such beetles [22].

2.1 Liquid crystal thermography

TLCs can be painted or airbrushed onto a surface to measure the wall temperature response or can be suspended in a fluid acting as thermal tracers. By dispersing the liquid crystals they can also be used as particles for flow visualization and measurements, thereby obtaining simultaneous information on temperature and velocity. This kind of particle image velocimetry/thermometry has received increasing attention in the last decade [7, 23, 24] as well as scanning techniques to visualize the three-dimensional temperature fields [25].

Figure 3 shows the results obtained with unencapsulated TLC tracers for visualization of natural convection in a differential heated cube-shaped cavity [26]. Using multi-exposed colour photographs, the flow traces as well as the temperature fields are obtained. Other applications of this technique include thermocapillary flows, heated vortex rings and natural convection with solidification. Usually, the flow velocities are rather small in these cases.

Visualizing the temperature field in a fluid flow at larger velocities was done by the application of fine nylon meshes placed in the flow. These meshes were sprayed with TLCs to reflect the temperature field in the flow [27, 28]. For internal flow situations, wide-band TLCs were used to infer the homogeneity of the temperature over a cross section. Narrow-band TLCs were used to measure individual isotherms in film-cooling applications. To obtain more information two narrow-band TLCs with different colour ranges were used. In addition, the temperature field generated by a cold jet into a hot main flow could be visualized and measured.

Figure 2: Exocuticles of a beetle containing chitin layers that possess a cholesteric liquid crystal structure (from [22], © David C. Hawks).

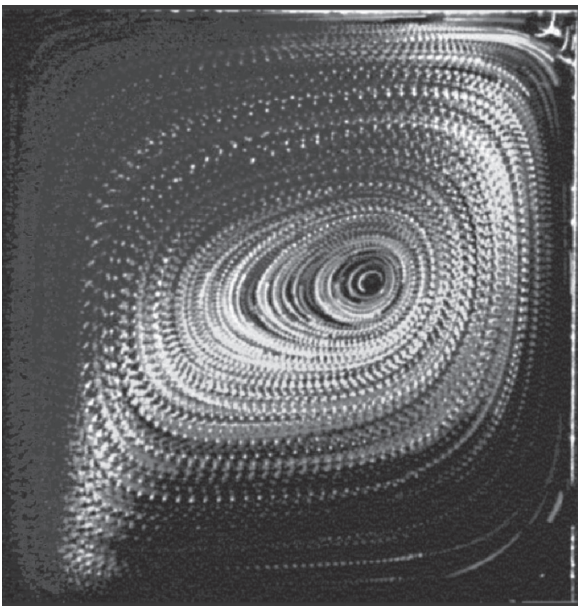

Figure 3: Multi-exposed colour photograph of convective flow seeded with liquid crystal tracers (from [26]).

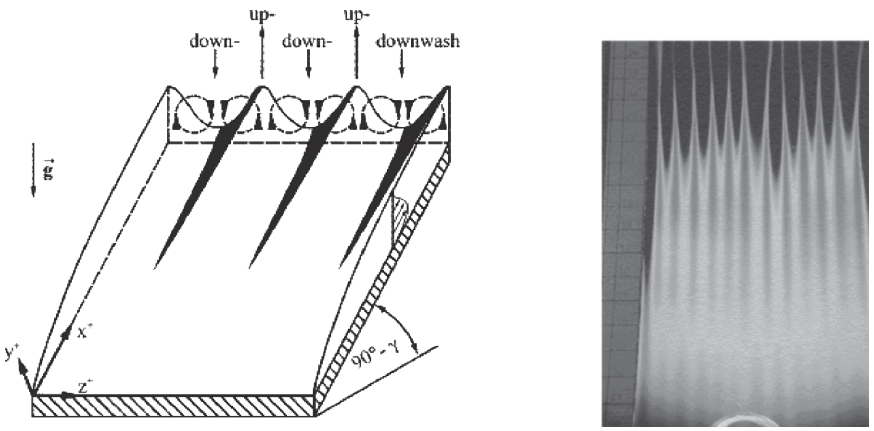

Figure 4: Longitudinal vortices in laminar natural convection along a heated inclined flat plate (left) and liquid crystal wall temperature visualization (right) (from [29]).

Surface thermography using wide-band liquid crystals has been applied to many problems in natural and forced convection situations. An example is given in Fig. 4, where the effect of longitudinal vortices in a laminar natural convection boundary layer flow along a heated inclined flat plate is visualized [29]. The two-dimensional boundary layer becomes unstable due to three-dimensional disturbances in the form of streamwise oriented, counter-rotating vortices as shown on the left in Fig. 4.

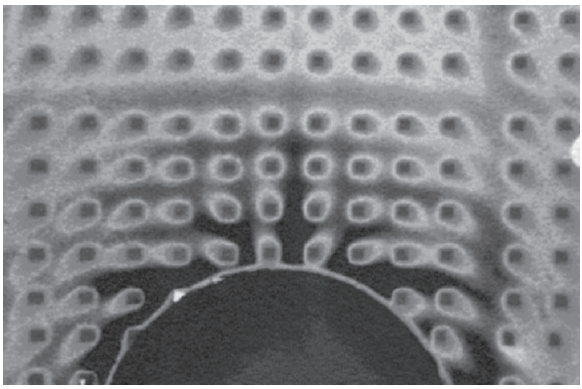

Figure 5: Spot visualization of flow around a cylinder using wide-band liquid crystals (from [30]).

The up- and downwash motions of the vortices influence the local heat transfer characteristics leading to a periodic temperature pattern on the constant heat flux surface. Dark indications show colder regions which correspond to higher heat transfer.

A turbulent forced convection flow situation is visualized in Fig. 5 using the flow field around a circular cylinder in a turbulent boundary layer [30]. Small heated spots on the bottom wall are generated using an aluminium pin fin arrangement. The applications of the TLC allows the detection of thermal wakes from each heated spot which will influence the downstream thermal conditions.

2.2 Calibration

For quantitative temperature measurements, calibration of the TLC is necessary. Although the colour play of narrow-band TLCs is usually within 1–1.5 K, for precise data, often accuracies of 0.1–0.2 K are needed. This requirement becomes more pronounced if wide-band TLCs (colour play within 5–25 K) are used.

Several techniques can be applied for establishing the temperature–colour relationship of the TLC [31–34]. In a typical TLC application, the surface to be observed is illuminated with a white light source. Colour images are taken and digitized to a RGB (red–green–blue) format, which can be related to the HSI (hue-saturation-intensity) space [33, 35], which is based on human colour reception.

There are two main techniques related to the band of the TLC. The narrow-band technique uses a single event colour as indicator for a certain temperature. Generally 'yellow' is chosen, because it has the narrowest temperature range [36]. Similarly, the highest intensity signal can be used [37], which is usually in the 'yellow' to 'green' range. This technique can also be used for monochrome cameras. A typical calibration example is given in Fig. 6. With this method, only a single calibration point is needed.

The wide-band technique establishes a hue–temperature relationship over the full range of displayed TLC colours using the hue angle [32, 38, 39] or the intensity history [34], which can be applied to colour as well as monochrome processing procedures.

The hue vs. temperature calibration depends on the viewing and lighting angles, especially for wide-band liquid crystals [33, 38], which needs to be taken into account. Aligning both, the viewing and the lighting axes provide thereby the least sensitivity. For highly curved surfaces

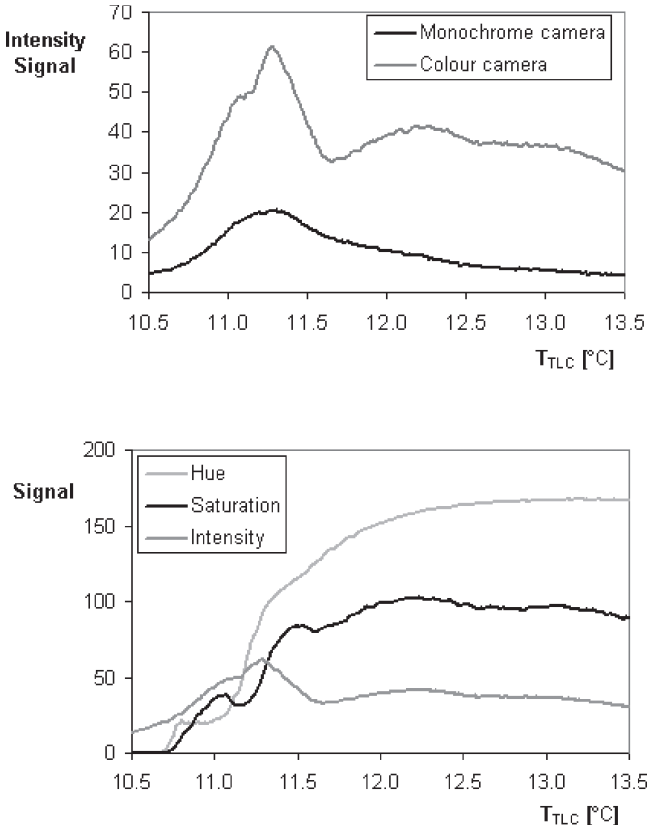

Figure 6: Calibration signals using colour or monochrome cameras, TLC BM/R10.5C1W/C17-10 from Hallcrest Ltd^{TM}.

the viewing/illumination angle should be taken as a parameter in the calibration curve [40]. For measurements on complex, curved surfaces using wide-band liquid crystals, special computer-controlled mini-calibrators were developed [41] using Peltier devices and thermoelectric coolers. These calibrators can be used for *in situ* calibration thereby achieving the same viewing and lighting conditions for calibration as well as for measurements. If periodic heating of the investigated surface or on–off heating conditions are used in heat transfer measurements [42, 43], hysteresis effects need to be considered. Hysteresis in liquid crystal behaviour might arise if they are overheated well above the upper clearing point [44].

Narrow-band TLCs have the advantage that, due to the smaller temperature band, the influence of viewing and lighting conditions is limited. Usually, these TLCs can be accurately calibrated to less than 10% of their colour band, i.e. less than 0.1 K. On the other hand they can be used over a small temperature range only. For full surface thermography, wide-band TLCs are better suited.

An intermediate approach is to use a mixture of several narrow-band TLCs indicating colours within different temperature ranges, by which several discrete isotherms can be visualized on the surface. An example is given in Fig. 7 for a film-cooling situation. Cold fluid enters the mainstream via jets from discrete holes and mixes with the hot gas flow. The effect of the mixing can be observed on the wall, which is made of a plastic material to behave nearly adiabatically.

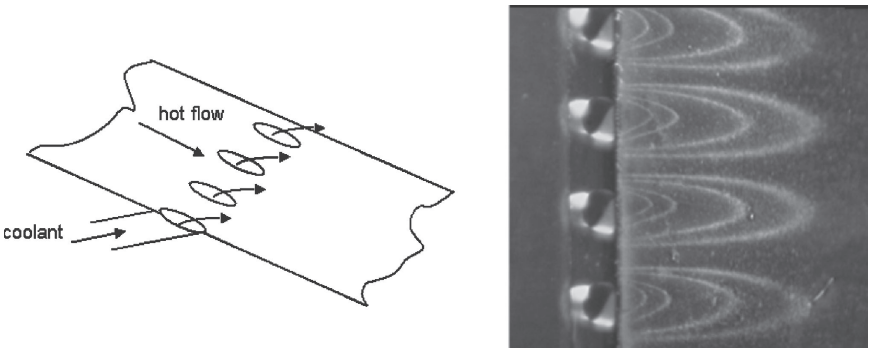

Figure 7: Sketch of film-cooling situation and image from a multiple narrow-band TLC mixture.

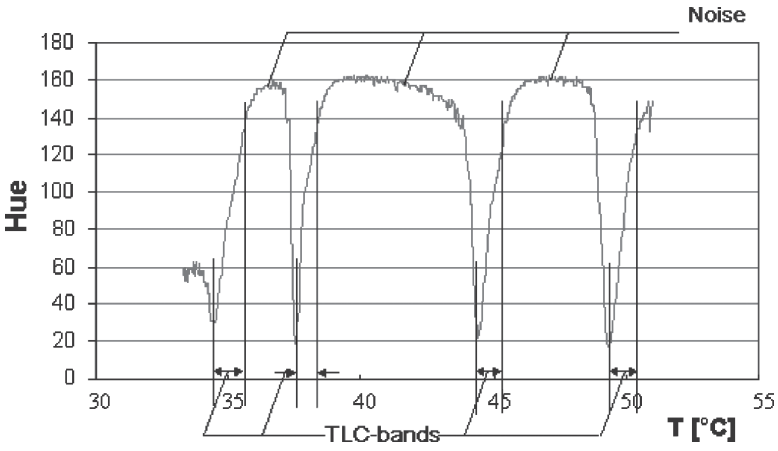

Figure 8: Hue–temperature calibration curve for a mixture of four narrow-band liquid crystals (from [45]).

The isotherms shown by the TLCs are therefore a measure of the local mixing temperature. Four different narrow-band TLCs were used here, which have their colour play within a temperature range of ∼1 K and response temperatures between the cold and the hot gas temperatures. To detect possible interference effects between the individual TLCs, they should be mixed before and the coating and calibration should be done later with the mixture. A typical mixture calibration curve is given in Fig. 8 for the hue value vs. temperature [45]. The ranges for the individual TLCs are clearly seen.

2.3 Heat transfer measurement techniques

TLCs are very helpful for the visualization of local heat transfer phenomena. For quantitative heat transfer measurements two main techniques have been established. Overviews about these methods and their history are given and by Ireland and Jones [6] Ekkad and Han [10]. The so-called steady-state technique employs a constant heat flux on the model surface by thin electrically heated foils and monitors the surface temperature by TLCs. Knowing the local heat flux and the

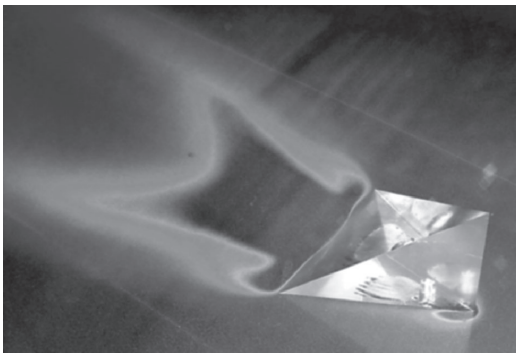

Figure 9: Liquid crystal image for flow around a vortex generator using a heated metallic foil.

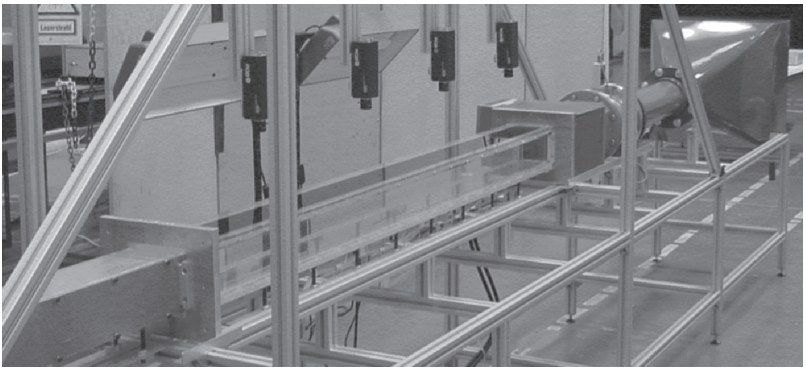

Figure 10: Typical set-up for liquid crystal heat transfer measurements using the transient technique.

temperature difference between the model surface and the fluid, the local heat transfer coefficient can be deduced. A typical liquid crystal pattern for the flow around a three-dimensional vortex generator is shown in Fig. 9. The bottom wall experiences a constant heat flux using a thin electrically heated stainless steel foil. The foil is covered with a thin layer of black paint on which the TLCs are applied. Narrow-band TLCs are used to map the colours of certain isotherms, corresponding in this case to lines of constant heat transfer coefficients. The location of the isotherms on the test wall can be changed by adjusting the actual heating level.

In the transient technique a sudden change in the thermal boundary conditions is applied in many cases by changing the fluid flow temperature rapidly [6] or by switching heated foils [46]. For this several methods have been proposed, like pre-heating or pre-cooling the model including rapid insertion mechanisms, switching valves, shroud techniques or fine electrically heated meshes [47, 48]. A typical test set-up for the heated mesh technique is shown in Fig. 10. The test section is simultaneously monitored with several CCD cameras. The air flow is sucked through the inlet filter on the right and heated suddenly by an electrical mesh heater before entering the test channel.

The change in the thermal boundary conditions due to the heated flow initiates a transient heat exchange and isotherms 'move' over the TLC-coated model surface. The TLC indication temperature is between the initial wall temperature and the hot flow temperature. Taking into

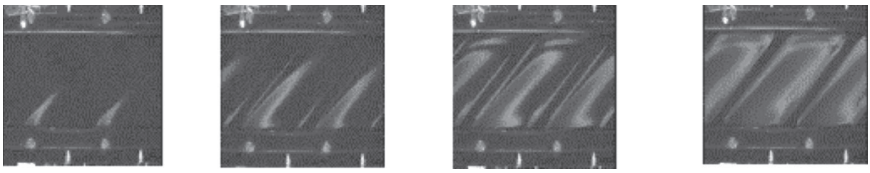

Figure 11: Time sequence (from left to right) of liquid crystal appearance in a transient experiment.

account typical measurement uncertainties for time, temperature and thermal properties, the TLC temperature should be selected to be approximately between the other two [49]. In case of a heated flow relative to the model initial temperature, early TLC indications (fast surface heating) indicate high heat transfer rates, while later TLC appearance (slow surface heating) reflects low heat transfer. With this, the thermal effects of recirculation zones, secondary flows, longitudinal vortices or separation and reattachment phenomena can be observed quite well. Figure 11 shows a time sequence of the TLC observation for a suddenly heated flow in a square channel with square ribs aligned at 45° with respect to the main flow.

Using appropriate conduction/convection analysis models for the solid test wall, quantitative distributions of the heat transfer coefficients can be calculated. These models are based on the assumption of low-conducting semi-infinite walls including possible time variations in the fluid flow temperature [10, 47], which are especially important in long cooling channels [50, 51], wall thickness and curvature effects [52]. Perspex is almost always chosen, because of its good optical properties, low conductivity and easy manufacturability.

3 Pressure Sensitive Paints (PSPs)

In a large number of applications in aerodynamic testing or basic fluid mechanics research, pressure measurements play a fundamental role. Besides the more conventional method of using pressure taps and transducers, PSPs are being increasingly used as an optical measurement method for full surface information. With pressure data available over the full surface and not only at discrete points, effects of flow separation, reattachment or shock locations can immediately be identified. Therefore PSPs make it easily possible to gain information on the effect of changed flow situations, whereas pressure tap instrumentation is usually optimized for only few special flow conditions. Having the pressure information on the full surface and integrating allows further determination of forces and moments on a model. The use of PSPs for pressure measurements is repeatable as long as they do not change too much (e.g. by photodegradation). The investigation of PSPs started in the early to mid-1980s. Details of these developments and the history can be found in several reviews [53–57].

The measurement process is based on the deactivation of excited molecules by collision with oxygen molecules (quenching) and the resultant reduced deactivation by light emission (photoluminescence). The quenching of luminescence by oxygen of organic molecules in a solution was discovered in 1935 by Kautsky and Hirsch [1]. Peterson and Fitzgerald [58] applied the oxygen quenching of fluorescence for surface flow visualization using nitrogen and pure oxygen streams near the surface in an air flow. Wilson *et al*. [59] used the oxygen-dependent quenching of phosphorescence for animal tissue investigations. Other applications include sensors to determine the oxygen content in inspired or expired gases, which were used to study the behaviour of bronchial systems [60], for mapping of oxygen distribution in biological samples [61] or intracellular oxygen measurements [62].

3.1 Photoluminescence

The basic principle of PSPs for pressure measurements is based on the photoluminescence process of some substances, called luminophores. When the molecules of such substances are illuminated with light of a particular wavelength they absorb energy and are excited from the base energy state (S_0) to a higher energy state (S_1). The energy states have different quantized levels (electron, vibration and rotation levels). The higher energy level can be lost by emission of light (luminescence) of a different, usually longer, wavelength or without radiation.

Generally, most of the molecules are in their ground-state energy level S_0. The absorption of light of appropriate energy and the implied excitation of a molecule M can be written as

$$M_{S_0} + h\nu \rightarrow M_{S_1}, \tag{1}$$

where h is Planck's constant and ν is the frequency of the absorbed light. Through non-radiative processes the excited molecule can reach the lowest excited level of S_1, which has the longest lifetime and is called the fluorescent state. From this point on, the luminophore may undergo different processes. Radiationless relaxation to the ground state may occur by conversion of vibrational, rotational and translation energy to heat.

$$M_{S_1} \rightarrow M_{S_0} + \text{heat}. \tag{2}$$

Intersystem crossing might occur, where one of the electrons changes the spin direction and transfers from the singlet state (S) to the triplet state (T). Triplet states form their own set of excited states. The radiative transition from T_1 to the ground state S_0 is spin-forbidden and much slower than the radiative transition between singlet states with the same spin number. This type of emission is called phosphorescence.

$$M_{T_1} \rightarrow M_{S_0} + h\nu_{\text{ph}}. \tag{3}$$

The most relevant conversions for the application as PSPs happen between the lowest singlet excited state S_1 and the ground state S_0. The two competing processes are the radiative deactivation by emission of fluorescent light

$$M_{S_1} \rightarrow M_{S_0} + h\nu_{\text{fl}} \tag{4}$$

and the non-radiative deactivation by oxygen, the so-called oxygen quenching.

$$M_{S_1} + O_2 \rightarrow M_{S_0} + O_2^*. \tag{5}$$

More detailed descriptions on these processes and further references can be found in the aforementioned reviews [53–57]. For a given molecule all these processes occur at a specific rate. The inverse of this rate represents the time constant or lifetime. Non-radiative processes, with the rate k_{w} elapse typically in $1/k_{\text{w}} = 10^{-9}$ s. Fluorescence with the rate k_{fl} has approximately the same lifetime, whereas the lifetime for phosphorescence with the rate k_{ph} is much longer and lies typically between 10^{-6} s and several seconds.

3.2 Measurement concept

PSP formulations currently used in wind tunnel testing typically consist of two or more layers, as presented in Fig. 12 [54]. The screen layer, a special white paint, provides optical uniformity of the surface and promotes reflection of both unabsorbed excitation and emission back through the

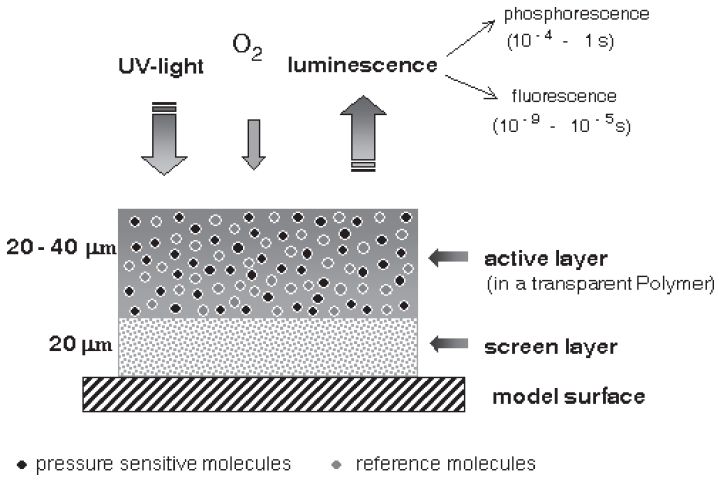

Figure 12: Layers of PSP coating on a model surface (from [54]).

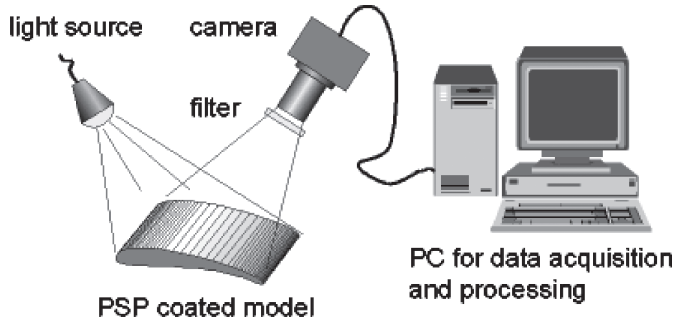

Figure 13: Schematic presentation of the PSP measurement concept (from [63]).

polymer layer. The contact layer ensures adhesion between the screen and the polymer layer. The polymer layer is the active layer containing photoluminescent molecules. This layer can consist of several components including a binder material, which needs to be highly permeable to oxygen. In Fig. 12, a 'binary paint' is shown, including pressure-sensitive luminophores and intensity-sensitive luminophores, which are used for intensity corrections in case of non-homogeneous illumination conditions [54]. The measurement concept of PSPs is presented in Fig. 13 [63]. The coated model is illuminated with light of appropriate energy to excite the luminophores. When relaxing to the ground state, light with a lower frequency than that required for excitation is emitted. The resulting luminescence is detected using a CCD camera, equipped with optical filters that allow only emitted light to pass. Further processing of the images is usually carried out using a personal computer. The luminescence intensity depends on the oxygen concentration. If a gas flow of known oxygen content (e.g. air) is used, the local oxygen concentration (partial pressure) is directly related to the local gas pressure. This behaviour is described by the Stern–Volmer relation [53, 54], which can be given in the form

$$\frac{I_0}{I} = a(T) + b(T)\frac{p}{p_0}, \tag{6}$$

where I_0 is a reference intensity at pressure p_0 (i.e. maximum intensity in the absence of a quencher or at known conditions). The coefficients a and b have to be determined by calibration and should take into account possible dependencies on temperature. This linear relationship is sometimes extended to a second-order equation and expressed in the form of pressure as a function of intensity:

$$\frac{p}{p_0} = A(T) + B(T)\frac{I_0}{I} + C(T)\left(\frac{I_0}{I}\right)^2. \tag{7}$$

Besides the measurement image at flow conditions (wind-on), a reference image (wind-off), taken at known conditions with the flow completely stopped, is required. Often a so-called dark image without any illumination is also taken. It is subtracted from the other two images to remove any baseline offset due to thermally generated electrons, readout noise or stray light. The modified Stern–Volmer relation [see eqn (7)] is used to calculate the pressure field whereas the necessary coefficients are obtained experimentally by calibrating the paint for a certain pressure range. In practice, a paint sample is placed in a calibration chamber, where the luminescence intensity is measured as a function of the pressure. Where the facility allows controlled pressurization, it is preferably to carry out the calibration directly on the model in the test facility.

Different measurement procedures are applied using the intensity time decay and by determining the luminescence lifetime from at least two time-resolved images (lifetime method) or the intensity method described above. More details and discussions of the advantages and the disadvantages of these methods can be found in [53, 54].

3.3 Calibration

In order to calculate the pressure field, the behaviour of the fluorescence intensity as a function of the pressure has to be analysed first. Three different methods are known to calibrate PSPs and to obtain the necessary coefficients. Generally an external calibration chamber (see Fig. 14) is used that allows for both pressure and temperature variations [63].

For a paint sample Stern–Volmer plots are generated over a certain pressure range and at different temperatures. For each temperature the coefficients $A(T)$, $B(T)$ and $C(T)$ [see eqn (7)] are determined through a second-order polynomial fit of the calibration curve. The temperature dependence of these coefficients is described by a function of the form $A(T) = a_0 + a_1T + a_2T^2$.

It is important that the paint sample is coated together with the test object to eliminate variations in paint characteristics due to different environmental conditions or other influences, e.g. layer thickness.

If the test facility permits pressurization of the test section, it is preferable to calibrate the paint directly on the installed test object. This second method has the advantage that differences in paint properties between the calibration sample and the installed model are excluded and the individual set of coefficients, which is generated for each measurement point, automatically corrects the influence of the viewing angle. Furthermore, illumination and camera position are exactly the same for calibration and measurement run.

Kavandi *et al*. [55] describe a third method where the paint is calibrated *in situ* but without pressurizing the test section. For this case, the test model needs to be equipped with pressure taps whose pressure values are acquired simultaneously with the intensity image. The intensity ratios I_0/I at the locations of the pressure taps are then plotted versus these pressures in the form of a calibration curve, from which the calibration coefficients can be obtained as in the previously described methods. It is important to place pressure taps in regions of extreme pressures to

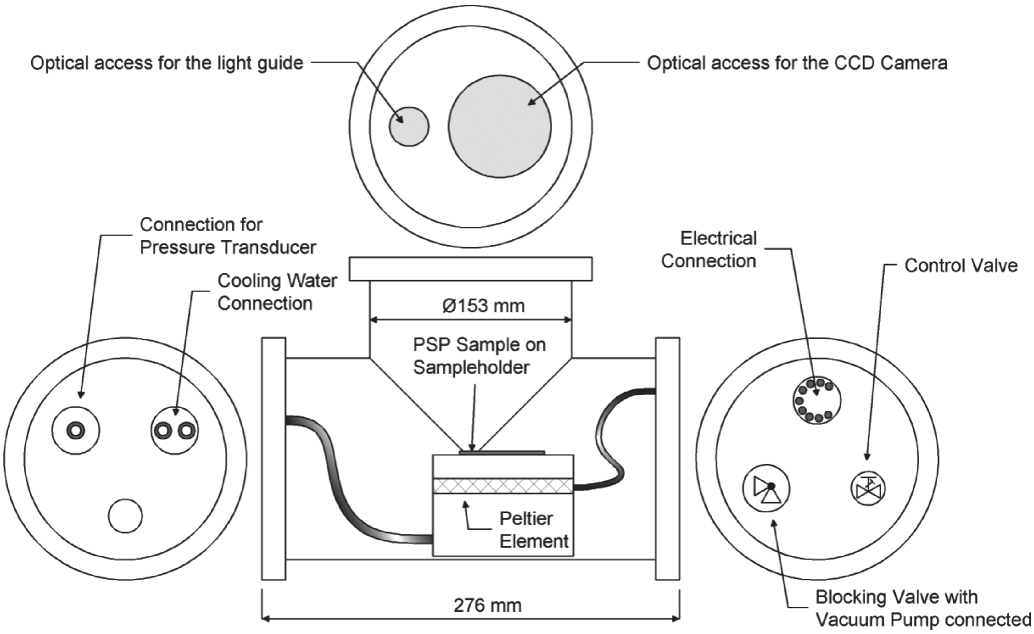

Figure 14: Calibration chamber (from [63]).

minimize any extrapolation of pressures from intensity ratios falling outside the calibration range. Moreover, it is also imperative that a number of taps are placed in locations between the pressure minima and maxima, so as to accurately define the shape of the calibration curve. It is also assumed that the temperature is the same over the whole model surface. This is important in the view that PSP formulations exhibit different temperature dependencies and sensitivities of the quenching rates with temperature [53, 64]. When large temperature effects are present on the model surface, simultaneous temperature measurements using, for example, IR thermography or thermocouples are needed.

3.4 Pressure measurements

Figure 15 shows the distribution of static pressure (here represented as isentropic Mach numbers) on the platform of a gas turbine vane passage [65]. A comparison with static pressure taps is also presented. The spatial resolution of the pressure taps is quite low. Only 29 pressure taps were distributed on the vane passage. The comparison shows clearly that the information gained with PSPs has a much higher resolution, while the comparison with the pressure tap values is very satisfactory. Uncertainties in the PSP measurement data arise from different sources such as non-uniformities of the polymer characteristics, very high levels of excitation light intensity, temperature dependence of the PSP and geometrical differences between the reference and the measurement images [63].

Recent works deal with 360° measurements of the pressure evolution on complete wind tunnel models. Engler *et al*. [66] and Klein *et al*. [67] describe such experiments. The model is observed simultaneously by several cameras. The detected pressure values are projected afterwards to a CFD surface mesh representing the model. In this way, the complete pressure evolution on the

model can be presented (Fig. 16). The integration of these pressures will then give the aerodynamic forces and moments on the model.

Further developments are directed towards very fast-reacting paint formulations, their application processes and the associated optical and electronic requirements for unsteady pressure measurements [68] taking into account the trade-off between steady signal-to-noise ratio and unsteady frequency response and the extension of PSPs to cryogenic environments [69].

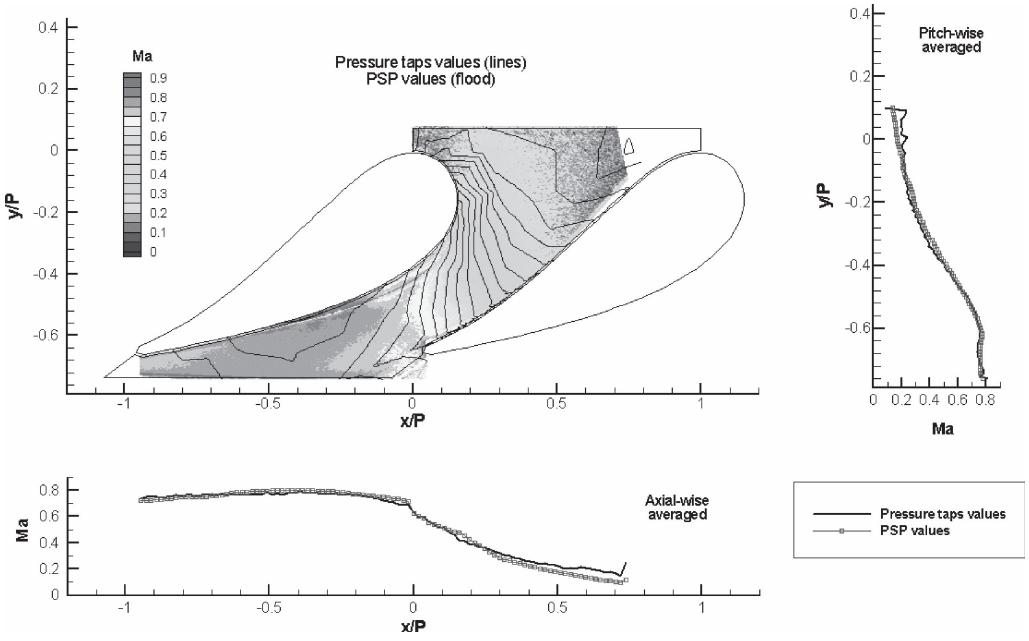

Figure 15: Comparison of Mach number distribution issued from PSPs (colours) and pressure taps (black contour lines) (from [65]).

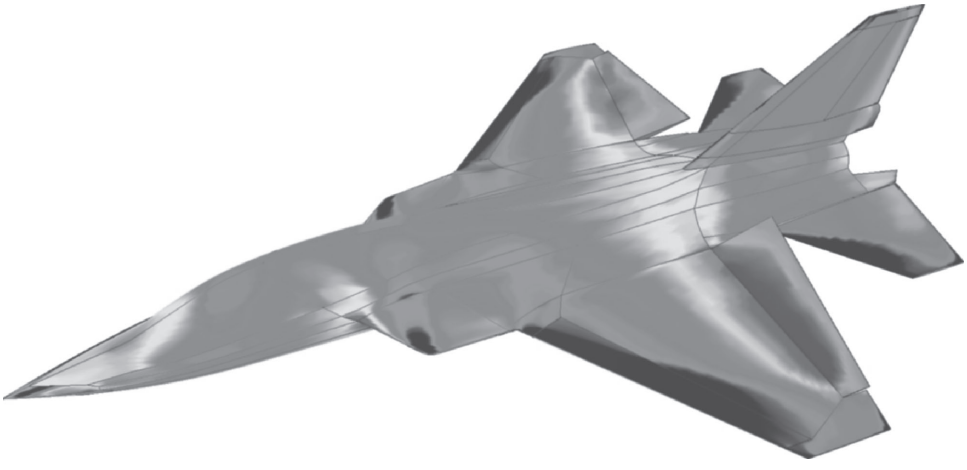

Figure 16: Integrated c_p values on the full model surface (from [67]).

3.5 Concentration measurements for film-cooling applications

The fact that the PSP measurement technique only works with a gas that contains oxygen can be used as an advantage to measure concentrations, i.e. the adiabatic film-cooling effectiveness of film-cooled turbine blades and platforms. The coolant is injected through holes and is supposed to form a film of cool gas thus protecting the metal against the extremely high temperatures in the main flow. This coolant film should stay attached to the wall and not mix too fast with the hot flow. By using a coolant gas without oxygen (i.e. N_2) during the tests, the concentration of oxygen and hence the mixing of the coolant with the main stream (air) can be visualized and measured. This allows for the determination of the effectiveness of the cooling scheme. This effectiveness η is defined as a dimensionless temperature ratio, which can be related to a concentration ratio using the analogy between heat and mass transfer [70, 71]. Thereby an adiabatic surface is required. Figures 17 and 18 show comparisons of the film-cooling effectiveness detected once by the

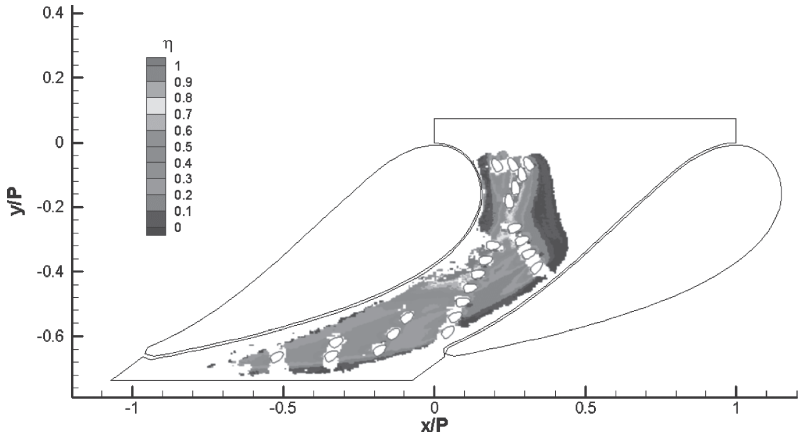

Figure 17: Film-cooling effectiveness distribution obtained using the transient liquid crystal technique (from [65]).

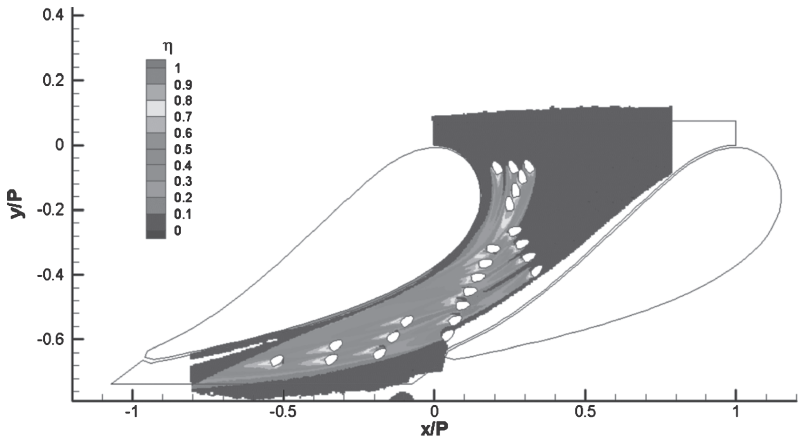

Figure 18: Film-cooling effectiveness distribution from PSPs with N_2 injection (from [65]).

transient liquid crystal method (Fig. 17) and once by the PSP technique (Fig. 18). The comparison shows that the PSP technique gives good results even close to the cooling holes, where the transient liquid crystal technique cannot obtain adiabatic conditions due to conduction processes towards the film-cooling hole. A combination of both techniques allows the improvement of the measurement accuracy as shown in [71, 72]. In this case, TLCs can help in determining the local recovery temperature and PSPs are applied for pressure measurements using air as the injected fluid. Nitrogen is then used for the injection and the film-cooling effectiveness distributions are obtained with the PSP on the adiabatic surface. Finally, the surface is heated and the heat transfer distributions measured using either the steady-state or the transient liquid crystal method.

Acknowledgements

The authors would like to thank IOP Publishing Ltd. for permission to use Figs 4 and 12, which have been published in [29] and [54], respectively. The authors acknowledge the permission of Springer for reprinting Fig. 5, which was published in [30], the permission of ASME to use Fig. 8, which was published in [45], and T. Kowalewski (Fig. 3), H. Beer (Fig. 4), R. Moffat (Fig. 5), R. Engler (Figs 12 and 16) for permission to use their results. We would like to thank S. Jacobs from the University of Rochester for directing us to the source of Fig. 2 and we gratefully acknowledge David C. Hawks for permission to use Fig. 2.

References

[1] Kautsky, H. & Hirsch, H., Detection of minutest amounts of oxygen by extinction of phosphorescence. *Zeitschrift für Anorganische and Allgemeine Chemie*, **222**, pp. 126–134, 1935.
[2] Parker, A.R., 515 million years of structural colour. *Journal of Optics A: Pure and Applied Optics*, **2**, pp. 15–28, 2000.
[3] Ireland, P.T. & Jones, T.V., The response time of a surface thermometer employing encapsulated thermochromic liquid crystals. *Journal of Physics E: Scientific Instruments*, **20**, pp. 1195–1199, 1987.
[4] Woodmansee, W.E., Aerospace thermal mapping applications of liquid crystals. *Applied Optics*, **7(9)**, pp. 1721–1727, 1968.
[5] Fergason, J.L., Liquid crystals in nondestructive testing. *Applied Optics*, **7(9)**, pp. 1729–1737, 1968.
[6] Ireland, P.T. & Jones, T.V., Liquid crystal measurements of heat transfer and surface shear stress. *Measurement Science and Technology*, **11**, pp. 969–986, 2000.
[7] Stasiek, J.A. & Kowalewski, T.A., Thermochromic liquid crystals applied for heat transfer research. *Opto-Electronics Review*, **10(1)**, pp. 1–10, 2002.
[8] Roberts, G.T. & East, R.A., Liquid crystal thermography for heat transfer measurement in hypersonic flows: a review. *Journal of Spacecraft and Rockets*, **33(6)**, pp. 761–768, 1996.
[9] Babinski, H. & Edwards, J.A., Automatic liquid crystal thermography for transient heat transfer measurements in hypersonic flow. *Experiments in Fluids*, **21**, pp. 227–236, 1996.
[10] Ekkad, S.V. & Han, J.C., A transient liquid crystal thermography technique for gas turbine heat transfer measurements. *Measurement Science and Technology*, **11**, pp. 957–968, 2000.
[11] Camci, C., Glezer, G., Owen, J.M., Pilbrow, R.G. & Syson, B.J., Application of thermochromic liquid crystal to rotating surfaces. *ASME Journal of Turbomachinery*, **120(1)**, pp. 100–103, 1998.

[12] Kenning, D.B.R., Kono, T. & Wienecke, M., Investigation of boiling heat transfer by liquid crystal thermography. *Experimental Thermal and Fluid Science*, **25**, pp. 219–229, 2001.
[13] Anbar, M., Gratt, B.M. & Hong, D., Thermology and facial telethermography. Part I: history and technical review. *Dentomaxillofacial Radiology*, **27**, pp. 61–67, 1998.
[14] Yang, W.J. & Yang, P.P., Literature survey on biomedical applications of thermography. *Biomedical Materials and Engineering*, **2**, pp. 7–18, 1992.
[15] Ashforth-Frost, S., Quantitative thermal imaging using liquid crystals. *Journal of Biomedical Optics*, **1**, pp. 18–27, 1996.
[16] Stasiek, J., Ciafalo, M., Tanda, G., Klosowicz, S., Zmila, J. & Kalicki, B., The use of thermochromic liquid crystals and image processing for technical and biomedical thermography. *Progress in Engineering Heat Transfer*, eds. B. Grochal, J. Mikielewicz & B. Sunden, IFFM Publishers: Gdansk, pp. 739–747, 1999.
[17] Romanovsky, A.A., Ivanov, A.I. & Shimansky, Y.P., Molecular biology of thermoregulation, selected contribution: ambient temperature for experiments in rats: a new method for determining the zone of thermal neutrality. *Journal of Applied Physiology*, **92**, pp. 2667–2679, 2002.
[18] Smith, W.K., Brodersen, C.R., Hancock, T.E. & Johnson, D.M., Integrated plant temperature measurement using heat-sensitive paint and colour image analysis. *Functional Ecology*, **18**, pp. 148–153, 2004.
[19] Srinivasarao, M., Nano-optics in the biological world: beetles, butterflies, birds, and moths. *Chemical Reviews*, **99**, pp. 1925–1961, 1999.
[20] Knight, D.P. & Vollrath, F., Liquid crystals and flow elongation in a spider's silk production line. *Proceedings of the Royal Society of London B*, **266**, pp. 519–523, 1999.
[21] Neville, A.C. & Caveney, S., Scarabaeid beetle exocuticle as an optical analogue of cholesteric liquid crystals. *Biological Reviews of the Cambridge Philosophical Society*, **44(4)**, pp. 531–562, 1969.
[22] Cave, R.D., Gleaming beetles from Central America attract insect enthusiasts and offer hope for saving & priceless habitat. http://www.nationalgeographic.com/ngm/0102/feature3/index.html
[23] Park, H.G., Dabiri, D. & Gharib, M., Digital particle image velocimetry/thermometry and application to the wake of a heated circular cylinder. *Experiments in Fluids*, **30**, pp. 327–338, 2001.
[24] Fujisawa, N. & Hashizume, Y., An uncertainty analysis of temperature and velocity measured by a liquid crystal vizualisation technique. *Measurement Science and Technology*, **12**, pp. 1235–1242, 2001.
[25] Lutjen, P.M., Mishra, D. & Prasad, V., Three-dimensional visualisation and measurement of temperature field using liquid crystal scanning thermography. *ASME Journal of Heat Transfer*, **123**, pp. 1006–1014, 2001.
[26] Kowalewski, T.A., Hiller, W.J. & de Vahl Davis, G., Computational and experimental visualization in heat and mass transfer problems. *First Japanese–Polish Joint Seminar in Computer Simulation*, Tokyo, eds. Akiyama, M., Kleiber, M. & Wolanski, P., pp. 60–69, 1994.
[27] Mee, D.J., Ireland, P.T. & Bather, S., Measurement of the temperature field downstream of simulated leading-edge film-cooling holes. *Experiments in Fluids*, **27**, pp. 273–283, 1999.
[28] Wang, Z., Ireland, P.T. & Kohler, S.T., Gas temperature measurement in internal cooling passages. *Proc. of the Int. Gas Turbine Conference*, Birmingham UK, ASME paper 96-GT-534, 1996.

[29] Jeschke, P., Biertümpfel, R. & Beer, H., Liquid-crystal thermography for heat-transfer measurements in the presence of longitudinal vortices in a natural convection flow. *Measurement Science and Technology*, **11**, pp. 447–453, 2000.
[30] Batchelder, K.A. & Moffat, R.J., Surface flow visualization using the thermal wakes of small heated spots. *Experiments in Fluids*, **25**, pp. 104–107, 1998.
[31] Smith, C.R., Sabatino, D.R. & Praisner, T.J., Temperature sensing with thermochromic liquid crystals. *Experiments in Fluids*, **30**, pp. 190–200, 2001.
[32] Hay, J.L. & Hollingsworth, D.K., Calibration of micro-encapsulated liquid crystals using hue angle and a dimensionless temperature. *Experimental Thermal and Fluid Science*, **18**, pp. 251–257, 1998.
[33] Farina, D.J., Hacker, J.M., Moffat, R.J. & Eaton, J.K., Illuminant invariant calibration of thermochromic liquid crystals. *Experimental Thermal and Fluid Science*, **9**, pp. 1–12, 1994.
[34] Wang, Z., Ireland, P.T. & Jones, T.V., An advanced method of processing liquid crystal video signals from transient heat transfer experiments. *ASME Journal of Turbomachinery*, **117**, pp. 184–189, 1994.
[35] Roesgen, T. & Totaro, R., A statistical calibration technique for thermochromic liquid crystal. *Experiments in Fluids*, **33**, pp. 732–734, 2002.
[36] Ireland, P.T. & Jones, T.V., The measurement of heat transfer coefficients in blade cooling geometries. *AGARD Conf. Proc. CP 390*, Bergen, 1985.
[37] Akino, N., Kunugi, T., Ichimiya, K., Mitsushiro, K. & Ueda, M., Improved liquid-crystal thermometry excluding human colour sensation. *ASME Journal of Heat Transfer*, **111**, pp. 558–565, 1989.
[38] Camci, C., Kim, K. & Hippensteele, S.A., A new hue capturing technique for quantitative interpretation of liquid crystal images used in convective heat transfer studies. *ASME Journal of Turbomachinery*, **114**, pp. 765–775, 1992.
[39] Fiebig, M., Behle, M., Schulz, K. & Leiner, W., Color-based image processing to measure local temperature distributions by wide-band liquid crystal thermography. *Applied Scientific Research*, **56**, pp. 113–143, 1996.
[40] Chan, T.L., Ashforth-Frost, S. & Jambunathan, K., Calibrating for viewing angle effect during heat transfer measurements on a curved surface. *International Journal of Heat and Mass Transfer*, **44**, pp. 2209–2223, 2001.
[41] Elkins, C.J., Fessler, J. & Eaton, J.K., A novel mini calibrator for thermochromic liquid crystals. *ASME Journal of Heat Transfer*, **123**, pp. 604–607, 2001.
[42] Baughn, J.W., Mayhew, J.E., Anderson, M.R. & Butler, R.J., A periodic transient method using liquid crystals for the measurement of local heat transfer coefficients. *ASME Journal of Heat Transfer*, **120**, pp. 772–777, 1998.
[43] von Wolfersdorf, J., Höcker, R. & Sattelmayer, T., A hybrid transient step-heating heat transfer measurement technique using heater foils and liquid-crystal thermography. *ASME Journal of Heat Transfer*, **115**, pp. 319–324, 1993.
[44] Anderson, M.R. & Baughn, J.W., Hysteresis in liquid crystal thermography. *ASME Journal of Heat Transfer*, **126**, pp. 339–346, 2004.
[45] Schnieder, M., Parneix, S. & von Wolfersdorf, J., Effect of showerhead injection on superposition of multi-row pressure side film cooling with fan shaped holes. *Proc. of the Int. Gas Turbine Conference*, Atlanta, Georgia USA, ASME paper 2003-GT-38693, 2003.
[46] Vogel, G., Graf, A., von Wolfersdorf, J. & Weigand, B., A novel transient heater-foil technique for liquid crystal experiments on film-cooled surfaces. *ASME Journal of Turbomachinery*, **125**, pp. 529–537, 2003.

[47] Ireland, P.T., Neely, A.J., Gillespie, D.R.H. & Robertson, A.J., Turbulent heat transfer measurements using liquid crystals. *International Journal of Heat and Fluid Flow*, **20**, pp. 355–367, 1999.

[48] Pape, D., Jeanmart, H., von Wolfersdorf, J. & Weigand, B., Influence of the 180° bend geometry on the pressure loss and heat transfer in a high aspect ratio rectangular smooth channel. *Proc. of the Int. Gas Turbine Conference*, Vienna, Austria, ASME paper 2004-GT-53753.

[49] Yan, Y. & Owen, J.M., Uncertainties in transient heat transfer measurements with liquid crystal. *International Journal of Heat and Fluid Flow*, **23**, pp. 29–35, 2002.

[50] Chyu, M.K., Ding, H., Downs, J.P., Van Sutendael, A. & Soechting, F.O., Determination of local heat transfer coefficient based on bulk mean temperature using a transient liquid crystals technique. *Experimental Thermal and Fluid Science*, **18**, pp. 142–149, 1998.

[51] von Wolfersdorf, J., Höcker, R. & Hirsch, C., A data reduction procedure for transient heat transfer measurements in long internal cooling channels. *ASME Journal of Heat Transfer*, **120**, pp. 314–321, 1998.

[52] Wagner, G., Kotulla, M., Ott, P., Weigand, B. & von Wolfersdorf, J., The transient liquid crystal technique: Influence of surface curvature and finite wall thickness. *ASME Journal of Turbomachinery*, **127**, pp. 176–182, 2005.

[53] Bell, J.H., Schairer, E.T., Hand, L.A. & Mehta, R.D., Surface pressure measurements using luminescent coatings. *Annual Review of Fluid Mechanics*, **33**, pp. 155–206, 2001.

[54] Engler, R.H., Klein, C. & Trinks, O., Pressure sensitive paint systems for pressure distribution measurements in wind tunnels and turbomachines. *Measurement Science Technology*, **11**, pp. 1077–1085, 2000.

[55] Kavandi, J., Callis, J., Gouterman, M., Khalil, G., Wright, D., Green, E., Burns, D. & McLachlan, B., Luminescent barometry in wind tunnels. *Review of Scientific Instruments*, **61(11)**, pp. 3340–3347, 1990.

[56] McLachlan, B.G. & Bell, J.H., Pressure-sensitive paint in aerodynamic testing. *Experimental Thermal and Fluid Science*, **10**, pp. 470–485, 1995.

[57] McLachlan, B.G., Kavandi, J.L., Callis, J.B., Gouterman, M., Green, E., Khalil, G. & Burns, D., Surface pressure field mapping using luminescent coatings. *Experiments in Fluids*, **14**, pp. 33–41, 1993.

[58] Peterson, J.I. & Fitzgerald, R.V., New technique of surface flow visualization based on oxygen quenching of fluorescence. *Review of Scientific Instruments*, **51(5)**, pp. 670–671, 1980.

[59] Wilson, D.F., Rumsey, W.L., Green, T.J. & Vanderkooi, J.M., The oxygen dependence of mitochondrial oxidative phosphorylation measured by a new optical method for measuring oxygen concentration. *Journal of Biological Chemistry*, **263(6)**, pp. 2712–2718, 1988.

[60] Barnikol, W.K.R., Gaertner, Th., Weiler, N. & Burkhard, O., Microdetector for rapid changes of oxygen partial pressure (pO_2) during the respiratory cycle in small laboratory animals. *Review of Scientific Instruments*, **59(7)**, pp. 1204–1208, 1988.

[61] Holst, G., Kohls, O., Klimant, I., König, B., Kühl, M. & Richter, T., A modular luminescence lifetime imaging system for mapping oxygen distribution in biological samples. *Sensors and Actuators B*, **51**, pp. 163–170, 1998.

[62] Ji, J., Rosenzweig, N., Jones, I. & Rosenzweig, Z., Novel fluorescent oxygen indicator for intracellular oxygen measurements. *Journal of Biomedical Optics*, **7(3)**, pp. 404–409, 2002.

[63] Steiner, P., Application of the Pressure Sensitive Paint Technique to the Turbomachinery Environment. Dissertation Nr 2297, EPF-Lausanne, Switzerland, 2001.

[64] Schanze, K.S., Carroll, B.F., Korotkevich, S. & Morris, M.J., Temperature dependence of pressure sensitive paints. *AIAA Journal*, **35(2)**, pp. 306–310, 1997.
[65] Vogel, G., Experimental study on a heavy film cooled nozzle guide vane with contoured platforms. Dissertation Nr 2602, EPF-Lausanne, Switzerland, 2002.
[66] Engler, R.H., Klein, Chr., Merlo, E. & van Amerom, P., 360° PSP measurements in transonic flow. *19th ICIASF Congress*, Cleveland, Ohio, USA, pp. 149–158, 2001.
[67] Klein, Chr., Engler, R.H., Henne, U. & Sachs, W.E., Application of pressure sensitive paint (PSP) for determination of the pressure field and calculation of forces and moments of models in a wind tunnel. *12th International Symposium on Applications of Laser Techniques to Fluid Mechanics*, Lisbon, Portugal, 2004.
[68] Schairer, E.T., Optimum thickness of pressure-sensitive paint for unsteady measurements. *AIAA Journal*, **40(11)**, pp. 2312–2318, 2002.
[69] Asai, K., Amao, Y., Iijima, Y., Okura, I. & Nishide, H., Novel pressure-sensitive paint for cryogenic and unsteady wind-tunnel testing. *Journal of Thermophysics and Heat Transfer*, **16(1)**, pp. 109–115, 2002.
[70] Zhang, L.J. & Jaiswal, R.S., Turbine nozzle endwall film cooling study using pressure-sensitive paint. *ASME Journal of Turbomachinery*, **123**, pp. 730–738, 2001.
[71] Vogel, G., Wagner, G. & Bölcs, A., Transient liquid crystal technique combined with PSP for improved film cooling measurements. *The 10th Int. Symp. on Flow Visualization*, Kyoto Japan, F0109, 2002.
[72] Wagner, G., Vogel, G., Chanteloup, D. & Bölcs, A., Pressure sensitive paint (PSP) and transient liquid crystal technique (TLC) for measurements on film cooling performances. *The 16th Symp. on Measuring Techniques in Transonic and Supersonic Flow in Cascades and Turbomachines*, Cambridge UK, 2002.